RSC Advances

PAPER

View Article Online
View Journal | View Issue

Cite this: *RSC Adv.*, 2022, **12**, 28916

Naphthylisoindolinone alkaloids: the first ring-contracted naphthylisoquinolines, from the tropical liana *Ancistrocladus abbreviatus*, with cytotoxic activity†‡§

Shaimaa Fayez,[ab] Torsten Bruhn,[b] Doris Feineis,[a] Laurent Aké Assi,[c] Prem Prakash Kushwaha,[de] Shashank Kumar[d] and Gerhard Bringmann *[a]

Received 12th September 2022
Accepted 3rd October 2022

DOI: 10.1039/d2ra05758a

rsc.li/rsc-advances

The West African liana *Ancistrocladus abbreviatus* is a rich source of structurally most diverse naphthylisoquinoline alkaloids. From its roots, a series of four novel representatives, named ancistrobrevolines A–D (**14–17**) have now been isolated, displaying an unprecedented heterocyclic ring system, where the usual isoquinoline entity is replaced by a ring-contracted isoindolinone part. Their constitutions were elucidated by 1D and 2D NMR and HR-ESI-MS. The absolute configurations at the chiral axis and at the stereogenic center were assigned by using experimental and computational electronic circular dichroism (ECD) investigations and a ruthenium-mediated oxidative degradation, respectively. For the biosynthetic origin of the isoindolinones from 'normal' naphthyltetrahydroisoquinolines, a hypothetic pathway is presented. It involves oxidative decarboxylation steps leading to a ring contraction by a benzilic acid rearrangement. Ancistrobrevolines A (**14**) and B (**15**) were found to display moderate cytotoxic effects (up to 72%) against MCF-7 breast and A549 lung cancer cells and to reduce the formation of spheroids (mammospheres) in the breast cancer cell line.

Introduction

Ancistrocladus abbreviatus Airy Shaw (Ancistrocladaceae) is a woody liana native to the coastal rainforests of West Africa.[1–4] It is characterized by a plethora of structurally most diverse secondary metabolites belonging to the emerging class of naphthylisoquinoline alkaloids, with 280 as yet known representatives.[5–9] From this tropical plant, no less than 69 such compounds have so far been isolated, many of them with unique molecular scaffolds.[5,10–18] With 33 examples,[5,10,11,13,14,17] naphthyl*tetrahydro*isoquinoline alkaloids such as ancistrobrevine A (**1**), its 6-*O*-demethyl analogue **2**,[5,14] and ancistrobrevine D (**3**)[5,13] (Fig. 1) constitute the major portion of compounds produced by the plant. Their molecular moieties are coupled *via* their 5,1′-, 5,8′-, 7,1′-, or 7,8′-positions. In all these metabolites, the biaryl axis is rotationally hindered, due to the presence of mostly bulky *ortho*-substituents, leading to the phenomenon of atropisomerism.[5–7,19,20] Many of the alkaloids of *A. abbreviatus* are typical Ancistrocladaceae-type compounds (*i.e.*, with *S*-configuration at C-3 and an oxygen function at C-6), such as compounds **1–3**. But also metabolites with structural characteristics typical of alkaloids occurring in plants of the related Dioncophyllaceae family[21–23] were isolated, *viz.*, 3*R*-configured and lacking an oxygen function at C-6, such as dioncophylline A (**4**)[5,24,25] and its *N*-methyl analogue **5**.[5,10] Even mixed, hybrid-type compounds like ancistrobrevine M (**7**; 3*R*, 6-OH)[17] and dioncoline A (**6**; 3*S*, 6-H),[17] possessing the opposite characteristics, were discovered in the plant. *Ancistrocladus abbreviatus* is the only *Ancistrocladus* species known to contain naphthylisoquinoline alkaloids of all these four subclasses. Likewise reported was the occurrence of nine naphthyl*dihydro*isoquinolines,[5,12,14,15] six of which were 5,1′-coupled like ancistrobrevidine C (**8**),[15] which was highly effective against the aggressive and metastatic growth of pancreatic cancer cells. The outstanding metabolite pattern of *A. abbreviatus* also comprises a unique series of seven alkaloids with a non-hydrogenated

[a]*Institute of Organic Chemistry, University of Würzburg, Am Hubland, D-97074 Würzburg, Germany. E-mail: bringman@chemie.uni-wuerzburg.de*
[b]*Department of Pharmacognosy, Faculty of Pharmacy, Ain-Shams University, Organization of African Unity Street 1, 11566 Cairo, Egypt*
[c]*Federal Institute for Risk Assessment, Max-Dohrn-Str. 8-10, D-10589 Berlin, Germany*
[d]*Centre National de Floristique, Université d'Abidjan, Conservatoire et Jardin Botanique, Abidjan 08, Ivory Coast*
[e]*Molecular Signaling & Drug Discovery Laboratory, Department of Biochemistry, Central University of Punjab, Bathinda-151401, Punjab, India*

† Deceased on January 14, 2014.

‡ Dedicated to Professor Günther Heubl, Ludwigs-Maximilians-Universität München (LMU Munich) on the occasion of this 70th birthday.

§ Electronic supplementary information (ESI) available: Spectroscopic data include NMR (^{1}H, ^{13}C, ^{1}H, ^{1}H–COSY, HSQC, HMBC, NOESY, and ROESY), HRESIMS, IR, and ECD spectra of compounds **14–17** and GC-MSD chromatograms obtained from the oxidative degradation of **14–17**. See DOI: https://doi.org/10.1039/d2ra05758a

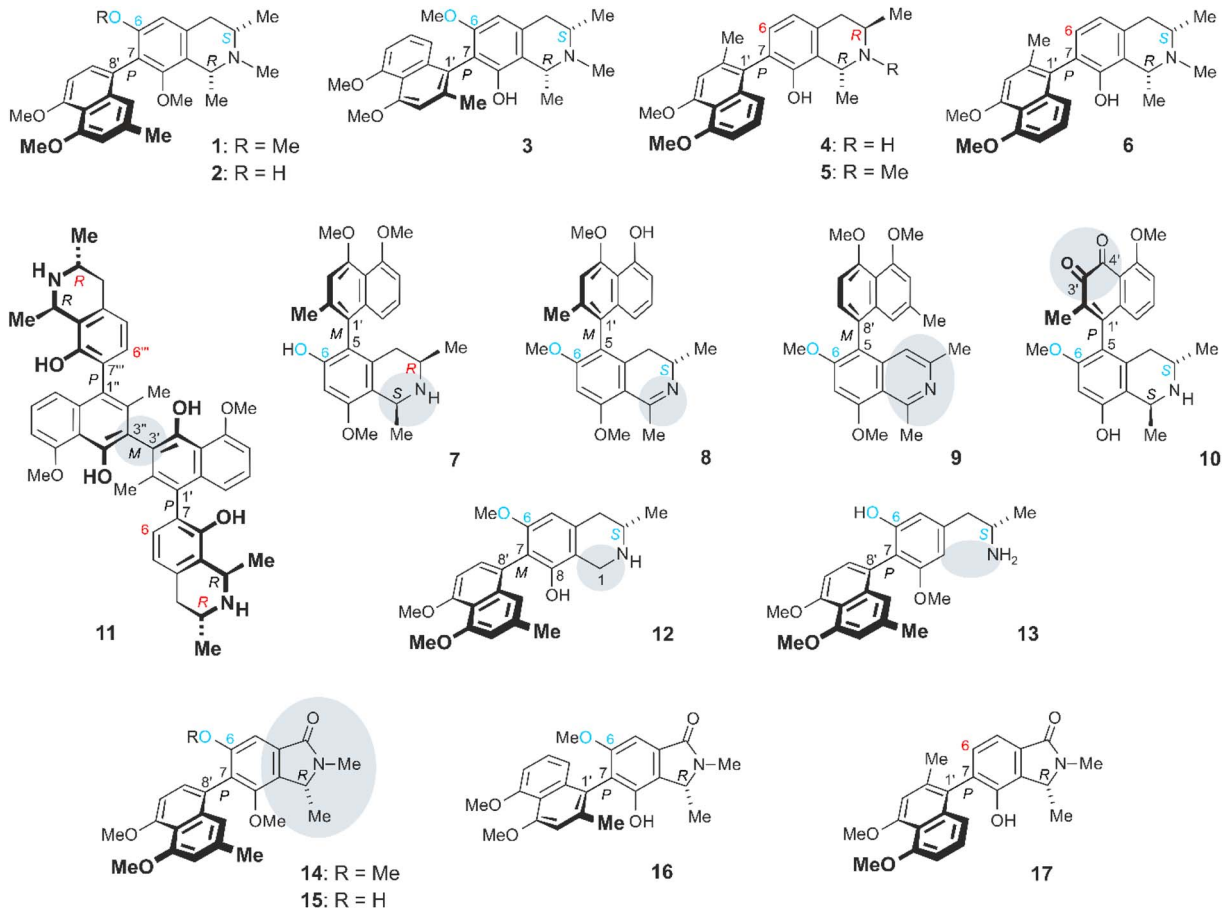

Fig. 1 Secondary metabolites produced by *A. abbreviatus*: the naphthyltetrahydroisoquinolines ancistrobrevine A (**1**) and its 6-*O*-methyl analogue **2**, ancistrobrevine D (**3**), dioncophylline A (**4**) and its *N*-methyl congener **5**, dioncoline A (**6**), and ancistrobrevine M (**7**), the dihydroisoquinoline ancistrobrevidine C (**8**), the non-hydrogenated ancistrobreveine D (**9**), the naphthoquinone derivative ancistrobreviquinone A (**10**), the dimer jozimine A_2 (**11**), the 1-unsubstituted 1-*nor*-8-*O*-demethylancistrobrevine H (**12**), the ring-cleaved ancistrosecoline D (**13**), and the novel ancistrobrevolines A–D (**14–17**). – Ancistrocladaceae-type alkaloids (with 6-OR and 3*S*) are labeled in "blue–blue", Dioncophyllaceae-type representatives (6-H and 3*R*) are marked in "red–red", the hybrid-type (6-OR and 3*R*) ancistrobrevine M (**7**) in "blue-red", and the only known[17] inverse-hybrid-type (6 H, 3*S*) dioncoline (**6**) in "red-blue".

isoquinoline part, from all four coupling types mentioned above, with the biaryl axis as the only stereogenic element, among them ancistrobreveine D (**9**).[16] Even though they are devoid of stereogenic centers, they are all optically active, occurring as enantiomerically pure compounds or as scalemic mixtures.[16] The broad spectrum of alkaloids produced by *A. abbreviatus* is further enlarged by the occurrence of dimeric congeners like the C_2-symmetric representative jozimine A_2 (**11**; both halves 7,1′-coupled). In the roots of *A. abbreviatus*, three further symmetric and unsymmetric dimers were detected, with the parent compound jozimine A_2 (**11**) being the most active agent against HT-29 colon cancer, HT-1080 fibrosarcoma, and MM.1S multiple myeloma cell lines.[17] Likewise isolated were quinoid structures like ancistrobreviquinone A (**10**),[15] possessing an *ortho*-naphthoquinone entity. Even more remarkable is the structure of the first 1-demethylated naphthylisoquinoline alkaloid, 1-*nor*-8-*O*-demethylancistro-brevine H (**12**),[18] lacking the otherwise generally present methyl group at C-1. This compound was isolated along with a series of unprecedented *seco*-alkaloids from the roots of *A. abbreviatus*,[18] having undergone a cleavage of the heterocyclic ring, with an elimination of the entire C-1/Me-1 unit, among them ancistrosecoline D (**13**) (Fig. 1). This alkaloid exerted potent, and selective, cytotoxicity against HeLa cervical cancer cells by inducing apoptosis.[18]

The 'chemical creativity' of *A. abbreviatus* is even larger, as shown in this report by the discovery of a series of metabolites constituting a novel subtype of axially chiral naphthyl*isoindolinone* alkaloids, named ancistrobrevolines A–D (**14–17**). In these compounds, the six-membered heterocyclic part of the isoquinoline portion has undergone a ring contraction to give a five-membered heterocycle as part of an isoindolinone system, with loss of the whole C-3/Me-3 entity, which had so far been present in all other naphthylisoquinoline alkaloids. For the origin of the novel naphthylisoindolinones **14–17** in the plants, a biosynthetic concept is presented, involving the stepwise loss of two carbon atoms and a benzilic acid rearrangement, leading to the observed ring contraction. Ancistrobrevolines A (**14**) and B (**15**) showed

moderate to good cytotoxic activities against lung and breast cancer cell lines.

Results and discussion

Isolation and structural elucidation of ancistrobrevolines A–D

Air-dried root bark material of *A. abbreviatus* collected in the Parc National de Taï in the Southwestern Côte d'Ivoire (Ivory Coast) was repeatedly extracted with MeOH. After filtration of the crude extract and evaporation of the solvent, the residual material was macerated with MeOH–H_2O (9 : 1, v/v), followed by liquid–liquid partitioning with *n*-hexane and fractionation by column chromatography on silica gel. HPLC-UV guided analysis of an alkaloid-rich fraction showed the presence of metabolites exhibiting UV spectra closely similar to those of naphthylisoquinoline alkaloids. They showed a first UV maximum at 224–229 nm, yet with an additional second UV maximum at 259–261 nm, resembling that of alkaloids with a fully dehydrogenated ring like ancistrobreveine D (**9**).

Ancistrobrevoline A (14). The first isolated compound had a molecular formula of $C_{25}H_{27}NO_5$, as indicated from its sodium adduct in HR-ESI-MS, $C_{25}H_{27}NNaO_5^+$, corresponding to *m*/*z* 444.17711 $[M + Na]^+$. The ^1H and ^{13}C NMR spectra (Table 1) showed predominantly signals typical of conventional naphthylisoquinoline alkaloids (Fig. 2A), in particular for the naphthalene part, with its usual 4′,5′-dimethoxy-2′-methyl substitution pattern, coupled *via* C-8′. The NMR data revealed a spin system with four aromatic methines, H-1′ (δ_H 6.70), H-3′ (δ_H 6.76), H-6′ (δ_H 6.92), and H-7′ (δ_H 7.16), a three-proton singlet ($\delta_{H,C}$ 2.29, 22.0) evidencing the presence of an aryl-methyl group (Me-2′), and further singlets for two methoxy functions, MeO-4′ ($\delta_{H,C}$ 3.92, 56.9) and MeO-5′ ($\delta_{H,C}$ 3.95, 56.7). The two aromatic singlets (δ_H 6.70 and 6.76) and an AB spin system of two adjacent protons (δ_H 6.92 and 7.16) indicated that the coupling site of the biaryl axis was located in the methyl-free part of the naphthalene moiety, *i.e.*, either at C-6′ or C-8′, which was in agreement with the normal, not highfield-shifted signal of Me-2′ (δ_H 2.29). The NOESY correlation sequence {MeO-5′ ↔ H-6′ ↔ H-7′} excluded the biaryl axis from being located at C-6′, thus establishing C-8′ to be the axis-bearing carbon atom. This assignment was confirmed by HMBC long-range couplings from H-1′ (δ_H 6.70) and H-6′ (δ_H 6.92) to C-8′ (δ_C 124.6), from H-7′ (δ_H 7.16) to C-9′ (δ_C 137.5), and from H-3′ (δ_H 6.76) to C-1′ (δ_C 118.8) (Fig. 2B).

Even the heterocyclic unit displayed, in part, the usual features as in other naphthylisoquinoline alkaloids, like the isocyclic benzene ring with the axis at C-7 (for the atom numbering applied, see ref. 26) and two methoxy functions at C-6 and C-8, as deduced from two singlets at δ_H 3.67 and 3.24, each corresponding to three protons, and from an aromatic singlet appearing at δ_H 7.21 (H-5) (Fig. 2A). The coupling pattern suggested the presence of a phenyl unit with no substituent at C-5, thus leaving C-7 (δ_C 128.1) as the axis-bearing carbon atom. This assumption was corroborated by HMBC interactions of H-5

Table 1 ^1H (600 MHz) and ^{13}C (150 MHz) NMR data of ancistrobrevolines A (**14**), B (**15**), C (**16**), and D (**17**) in methanol-d_4 (δ in ppm)

	14		**15**		**16**		**17**	
Position	δ_H (*J* in Hz)	δ_C	δ_H (*J* in Hz)	δ_C	δ_H (*J* in Hz)	δ_C	δ_H (*J* in Hz)	δ_C
1	4.69, q	58.4	4.65, q	58.3	4.58, q	58.3	4.67, q	58.5
4		169.8		169.9		170.4		170.3
5	7.21, s	101.2	7.05, s	105.4	7.01, s	97.4	7.37, d (7.6)	115.3
6		161.1		158.4		160.5	7.10, d (7.5)	133.6
7		128.1		126.7		120.5		131.9
8		155.6		155.8		151.9		151.5
9		132.6		131.0		128.2		135.3
10		134.0		133.9		133.8		133.6
1′	6.70, s	118.8	6.80, s	119.1		122.3		126.1
2′		137.3		137.9		137.9		137.2
3′	6.76, s	109.6	6.77, s	109.7	6.91, s	110.4	6.92, s	110.2
4′		158.4		158.4		158.2		158.2
5′		158.5		158.5		158.6		158.6
6′	6.92, d (8.0)	106.3	6.94, d (7.9)	106.4	6.85, d (6.9)	107.0	6.87, d (7.2)	107.0
7′	7.16, d (7.9)	130.3	7.22, d (7.9)	130.6	7.18, dd (7.8, 8.4)	127.6	7.19, dd (7.8, 8.4)	127.6
8′		124.6		124.6	6.81, dd (0.9, 8.4)	119.1	6.80, dd (0.9, 8.5)	119.5
9′		137.5		137.4		138.1		138.1
10′		117.1		117.3		117.8		117.8
1-Me	1.54, d (6.6)	17.2	3.20, d (6.6)	17.2	1.55, d (6.6)	16.8	1.58, d (6.6)	16.4
2′-Me	2.29, s	22.0	2.30, s	22.0	2.09, s	20.5	2.16, s	20.7
N–Me	3.15, s	27.1	3.13, s	27.1	3.14, s	27.3	3.15, s	27.2
6-OMe	3.67, s	56.5			3.64, s	56.3	3.64, s	
8-OMe	3.24, s	60.6	3.23, s	60.5				
4′-OMe	3.92, s	56.9	3.92, s	56.9	3.97, s	56.8	3.97, s	56.8
5′-OMe	3.95, s	56.7	3.96, s	56.7	3.92 s	56.9	3.91, s	56.9

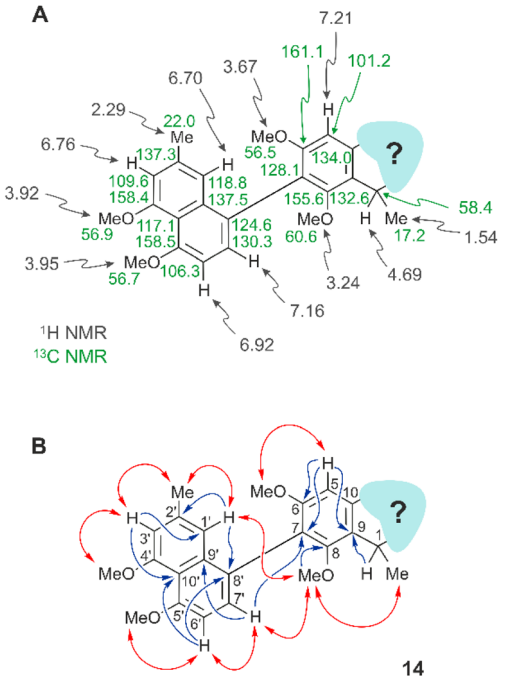

Fig. 2 1D and 2D NMR data of the naphthalene moiety and the phenyl part of the heterocyclic molecular half of ancistrobrevoline A (**14**) closely resembling those of conventional naphthylisoquinoline alkaloids, while the novel-type, yet unknown structural elements of **14** are overlaid in pale blue. (A) ^{1}H and ^{13}C NMR data (in methanol-d_4, δ in ppm). (B) HMBC (single blue arrows) and NOESY (double red arrows) interactions evidencing the constitution of the molecular units of **14** and the position of the biaryl axis between them. – For better comparability, the atom numbering follows the one usually applied for naphthylisoquinoline alkaloids.

(δ_H 7.21) to C-7 (δ_C 128.1) and C-9 (δ_C 155.6), and a ^{4}J correlation of C-7 with H-7′ (δ_H 7.16) across the biaryl axis (Fig. 2B). Likewise present was the usual CHMe entity at C-1, as seen from a quartet (H-1, δ_H 4.69) in the aliphatic region of the ^{1}H NMR spectrum, and from NOESY interactions between the protons of the methyl group appearing as a doublet at δ_H 1.54 and those of the OMe function at C-8 (δ_H 3.24), and between that *O*-methyl group and the two aromatic protons H-1′ (δ_H 6.70) and H-7′ (δ_H 7.16) (Fig. 2B), indicating that the methyl group at δ_H 1.54 was located at C-1 (δ_C 58.4), while the upfield-shifted OMe function resonating at δ_H 3.24 was at C-8 (δ_C 155.6).

The rest of the molecule, however, as overlaid in light blue (see Fig. 2 and structure **I** in Fig. 3), seemed substantially different from that of all other known naphthylisoquinoline alkaloids.

It was in particular the aliphatic region of the ^{1}H NMR spectrum that diverged massively from that of a usual naphthyltetrahydroisoquinoline alkaloid, characterized by the lack of resonances for the methyl group at C-3 (which normally appears around δ_H 0.9 and 1.3), the missing usual multiplet of H-3 in the region between δ_H 3.2 and 4.0, and the likewise absent signals of the diastereotopic geminal protons at C-4, which usually appear as doublets of doublets resonating around δ_H 1.7–3.2 (see structure **II** in Fig. 3). The observation of a downfield-shifted three-proton singlet (δ_H 3.15) suggested the presence of an *N*-methyl group, which was in accordance with the observation of a NOESY correlation to the protons of the methyl group at C-1 and with an HMBC interaction from the protons of that methyl group (resonating at δ_H 3.15) to the aliphatic carbon atom C-1 (δ_C 58.4) (see structure **III** in Fig. 3).

A further most notable difference compared to usual naphthylisoquinolines was the presence of an additional oxygen function in that eastern part of the molecule. The ^{13}C NMR data displayed a downfield-shifted signal at δ_C 170.0, typical of a carbonyl function. The observation of an HMBC cross-peak from the *N*-methyl group at δ_H 3.15 to that carbonyl *C*-atom, however, did not match with the structure of a six-membered tetrahydropyridinone as in structure **IV** (Fig. 3), since the distances between the two structural elements, *N*–Me and C-4, would have been two far for such an interaction.

The observed HMBC and NOESY interactions, while not fitting with the presence of an isoquinoline unit, gave conclusive evidence of a contracted ring in the new alkaloid, as a consequence of the loss of the carbon atom C-3, thus giving rise to a five-membered isoindolinone skeleton. This structural assignment presented in Fig. 3 (see structure **V**) was in agreement with the lack of the signal for C-3 in ^{13}C NMR (normally resonating at δ_C 45–53) and with the appearance of a signal at 1673 cm^{-1} in the IR spectrum, which is characteristic of a carbonyl group as part of an amide function. In conclusion, the new alkaloid had to be a 7,8′-coupled biaryl alkaloid, structurally differing from a conventional naphthylisoquinoline by its unprecedented isoindolinone part.

The absolute configuration at the stereocenter of the new alkaloid at C-1 in the isoindolinone ring system was determined by a ruthenium-mediated oxidative degradation procedure (see the ESI†) developed by us earlier.[6,27] Although this periodate oxidation method had initially been designed for the degradation of 1,3-disubstituted tetra- or dihydroisoquinolines, not for isoindolinones, with their stable C,N-bond, the reaction luckily succeeded in this case, too, affording the simple and easy-to-analyze chiral amino acid *N*-methyl-D-alanine, hence establishing the absolute configuration at the stereocenter as *R*.

Unfortunately, it was not possible to assign the configuration at the axis relative to the stereocenter at C-1 by NMR, because no significant long-range NOESY interactions across the biaryl axis were observed, like between Me-1 and/or H-1 in the isoindolinone ring and H-1′ or H-7′ in the naphthalene half. Apparently the small ring size of the heterocycle leads to enlarged distances between the substituent at C-1 and the respective H atoms attached to the naphthalene part. Therefore, quantum-chemical electronic circular dichroism (ECD) calculations were performed for both possible atropo-diastereomers.

The experimental ECD spectrum of the isolated naphthylisoindolinone (Fig. 4) was very similar to the one calculated for the *P*-isomer (in red) at the TDωB97XD3/def2-TZVP//B3LYP-D3/def2-TZVP level, while being virtually opposite to the one predicted for *M* (in blue), which unambiguously showed that the new compound was *P*-configured and, thus, had the full absolute stereostructure **14**, as presented in Fig. 1.

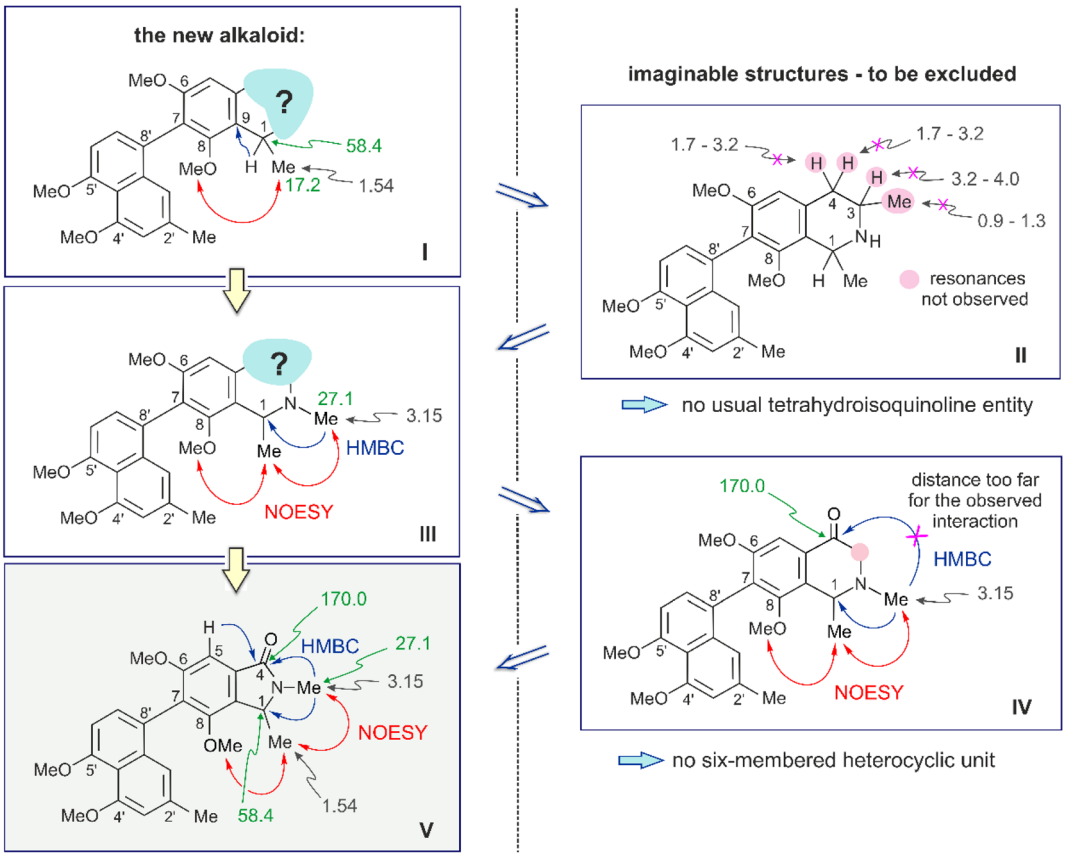

Fig. 3 Decisive ^{1}H and ^{13}C NMR shifts (in methanol-d_4, δ in ppm) and key NOESY (double red arrows) and HMBC (single blue arrows) interactions in structures I, III, and V, evidencing the structural elements of the heterocyclic ring in ancistrobrevoline A (**14**). The two geminal protons at C-4, the proton and the methyl group at C-3 (underlaid in pink in structure II), typical of usual naphthyltetrahydroisoquinoline alkaloids, were not observed in the ^{1}H NMR spectrum of **14**. Deletion of the carbon atom C-3 (marked in pink in structure IV) leads to the formation of the isoindolinone subunit of **14** as shown in structure V.

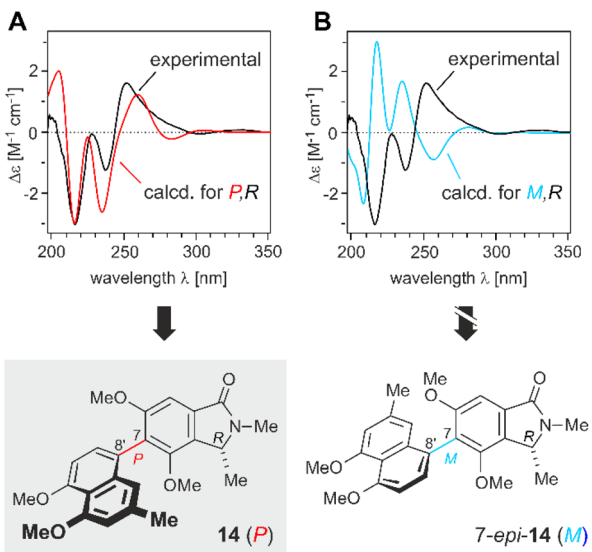

Fig. 4 Assignment of the absolute configuration of ancistrobrevoline A (**14**) by comparison of its experimental ECD spectrum (in black, taken in methanol) with the ones calculated (A) for the (1*R*,7*P*)-isomer (ECD curve in red) and (B) for 1*R*,7*M* (in pale blue) using TDωB97XD3/def2-TZVP//B3LYP-D3/def2-TZVP.

This novel natural product was given the name ancistrobrevoline A.

Ancistrobrevoline B (15). The second new minor root bark metabolite was spectroscopically almost identical to ancistrobrevoline A (**14**), with only slightly different chemical shifts (Table 1), thus evidencing the presence of another naphthylisoindolinone, again 7,8′-coupled, as attributed by the observed key HMBC and NOESY interactions (see the ESI†). The ^{1}H NMR spectrum displayed a three-proton singlet at δ_H 3.13, hinting at an *N*–Me group, and the ^{13}C NMR data revealed the presence of a downfield-shifted signal at δ_C 169.9, typical of the amidic carbonyl entity of the isoindolinone unit. This was in accordance with a carbonyl signal at 1678 cm^{-1} in the IR spectrum of the new metabolite. HR-ESI-MS showed a protonated molecular-ion peak $[M + H]^+$ at *m*/*z* 408.18150 (calcd for $C_{24}H_{26}NO_5^+$, 408.18055) and an $[M + Na]^+$ peak at *m*/*z* 430.16117 (calcd for $C_{24}H_{25}NNaO_5^+$, 430.16249), thus having 14 mass units less than 14, suggesting that the isolated new metabolite might be an *O*-demethylated analogue of **14**. In agreement with this assumption, the ^{1}H NMR spectrum displayed singlets for only three *O*-methyl units, resonating at δ_H 3.23, 3.92, and 3.96 (Table 1). They were assigned to be located at C-8, C-4′, and C-5′, based on NOESY interactions with Me-1/H-1, H-3′, and H-6′,

respectively, similar as for ancistrobrevoline A (**14**) (Fig. 2). Thus, different from **14**, one of the oxygen functions in the new metabolite was a free hydroxy group at C-6. The ECD spectrum of the new compound (see the ESI†) matched well that of ancistrobrevoline A (**14**), proving that the absolute configuration at the biaryl axis was again *P*, as for **14**. Likewise as in the case of **14**, the degradation[6,27] established the absolute configuration at the stereocenter at C-1 as *R* by the formation of *N*-methyl-D-alanine. The new alkaloid thus had the absolute stereostructure **15** as presented in Fig. 1, hence being the 6-*O*-demethyl analogue of **14**. It was named ancistrobrevoline B.

Ancistrobrevoline C (16). The third new compound was obtained as a yellow amorphous powder. According to HRESIMS and ^{13}C NMR, it had a molecular formula of $C_{24}H_{26}NO_5$, as deduced from its monoprotonated molecular ion, $[M + H]^+$, at *m*/*z* 408.17974, identical to that of ancistrobrevoline B (**15**). Again, the ^{1}H NMR spectrum showed signals for three *C*-methyl groups (δ_H 1.55, 2.09, and 3.14), for three methoxy functions (δ_H 3.64, 3.92, and 3.97), and for one aliphatic proton (δ_H 4.58) and five aromatic ones (δ_H 6.81, 6.85, 6.91, 7.01, and 7.18) (Fig. 5A). This, together with an IR band at 1675 cm^{-1} and a downfield-shifted signal at δ_C 170.4 in ^{13}C NMR, characteristic of an amidic carbonyl entity, indicated the new minor metabolite from the root bark of *A. abbreviatus* to be yet another naphthylisoindolinone alkaloid. Different from **15**, the new compound exhibited a spin pattern of the aromatic protons consisting of two singlets, one doublet, and two doublets of doublets. This was in agreement either with a 5,1′- or a 7,1′-coupling, of which the 5,1′-linkage was excluded due to HMBC interactions of H-5 (δ_H 7.01) to C-4 (δ_C 170.4) and C-7 (δ_C 120.5) and a NOESY correlation between H-5 and MeO-6 (δ_H 3.64) in the isoindolinone part (Fig. 5B). This assignment was confirmed by NOESY correlation sequences in the series {H-8′ ↔ H-7′ ↔ MeO-5′} and {MeO-4′ ↔ H-3′ ↔ Me-2′} and by HMBC cross-peaks of Me-2′ (δ_H 2.09) and H-8′ (δ_H 6.81) to C-1′ (δ_C 58.3) in the naphthalene moiety. The three methoxy groups were determined to be located at C-6, C-4′, and C-5′, based on NOESY interactions with their neighboring protons, H-5, H-3′, and H-6′, respectively (Fig. 5B). Another oxygenated carbon atom was found to be located in the phenyl ring, at C-8 (δ_C 151.9), bearing a free hydroxy function. The ruthenium-mediated oxidative degradation[6,27] of the new compound afforded the D-enantiomer of *N*-methylalanine, establishing the absolute configuration at the stereocenter as *R*.

The absolute axial configuration of the new alkaloid was deduced by comparison of its experimental ECD spectrum (full line in blue) with that of ancistrobrevoline A (**14**, dotted line in black). The new alkaloid differed from **14** only by the position of the methyl group in the naphthalene part or, in other words, by the coupling type (7,1′ *versus* 7,8′), and by the substitution pattern at C-6 and C-8 (OMe/OH *versus* OH/OMe in **14**). The ECD spectrum of the new alkaloid was virtually opposite to the one of **14** (Fig. 5D), suggesting that the larger part of the naphthalene unit should be directed down, *i.e.*, with an opposite stereoarray as compared to **14** and **15**. According to the Cahn-Ingold-Prelog priority rules, however, the descriptor was again assigned as *P*, *i.e.*, formally the same as for **14** and **15**. The new compound thus had the full stereostructure **16** as presented in Fig. 5D. It was named ancistrobrevoline C.

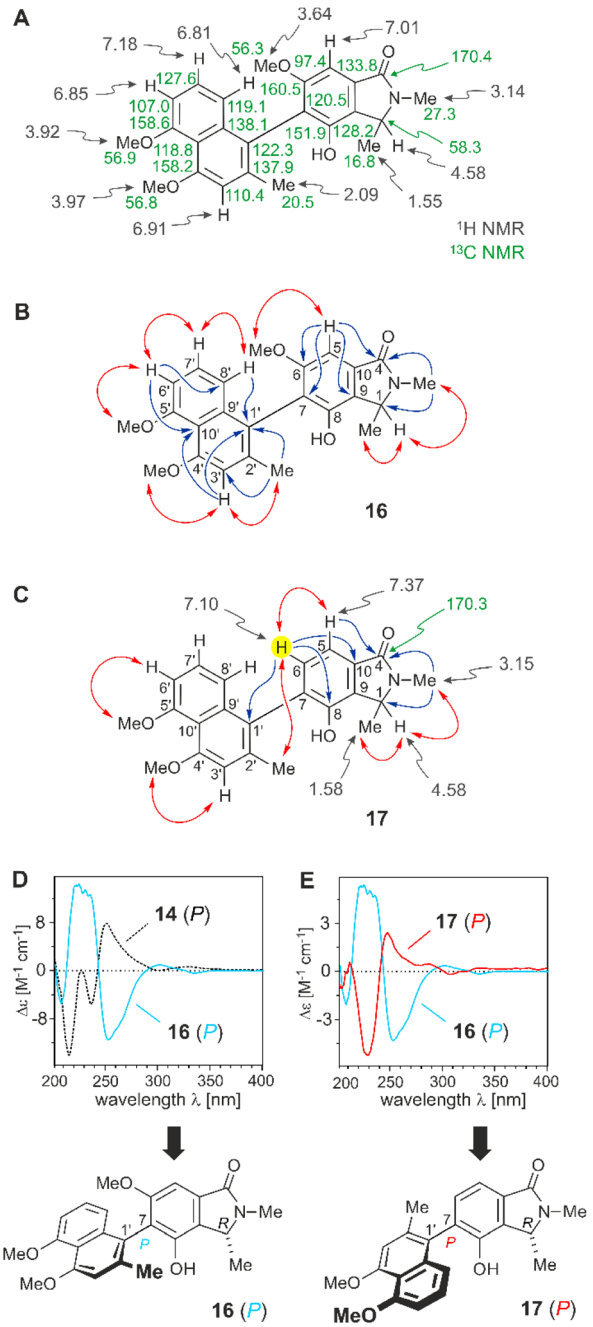

Fig. 5 (A) ^{1}H and ^{13}C NMR data (in methanol-d_4, δ in ppm) of ancistrobrevoline C (**16**). (B) Key HMBC (single blue arrows) and NOESY (double red arrows) interactions indicative of the constitution of **16**. (C) Decisive 1D and 2D NMR data of ancistrobrevoline D (**17**) evidencing the presence of an additional aromatic proton (highlighted in yellow). (D) Assignment of the absolute axial configuration in **16** by comparison of its experimental ECD spectrum (in pale blue, full line) with the ECD curve (in black, dotted line) of ancistrobrevoline A (**14**, for its structure, see Fig. 4). (E) Comparison of the ECD spectrum of **17** (in red, full line) with that of the likewise 7,1′-coupled ancistrobrevoline C (**16**) (in pale blue, full line).

Ancistrobrevoline D (17). The fourth compound was isolated as a yellow amorphous solid with a molecular formula of

$C_{23}H_{23}NO_4$, as established from the corresponding $[M + Na]^+$ adduct, $C_{23}H_{23}NNaO_4$, at *m*/*z* 400.15033. ^1H and ^{13}C NMR data (Table 1) revealed the new metabolite to be yet another 7,1′-linked naphthylisoindolinone alkaloid, with a constitution strongly resembling that of the above-described ancistrobrevoline C (**16**). Similar to **16**, it displayed a 4′,5′-dimethoxy-substituted naphthalene portion, as deduced by NOESY cross-peaks between MeO-4′ and H-3′ and between MeO-5′ and H-6′. Likewise observed in 1D and 2D NMR were the typical structural features of the heterocyclic ring in the isoindolinone moiety, as outlined in Fig. 5C. The molecular weight of the new metabolite, however, was lower than those of **14–16**, hinting at the presence of only four oxygen atoms. This gave rise to the assumption that the new alkaloid might be derived from the subclass of dioncophyllaceae-type compounds, which are characterized by the lack of an oxygen function at C-6 (and the presence of an *R*-configuration at C-3, which, however, does not apply here). Indeed, the most significant difference in the NMR spectrum of the new metabolite compared to that of **16** was the appearance of an additional aromatic proton, which was supposed to be the hydrogen atom at C-6. The coupling pattern of the aromatic protons showed one singlet (H-3′), two doublets (H-6′ and H-8′), and one doublet of doublets (H-7′) in the naphthalene part (Table 1), and two doublets resonating at δ_H 7.10 and δ_H 7.37, located in the isoindolinone portion. This assignment was in accordance with COSY interactions between H-5 (δ_H 7.37) and H-6 (δ_H 7.10), which showed *ortho*-coupling to each other (J = 7.5 Hz), and it was also confirmed by HMBC cross-peaks from H-6 to C-1' (δ_C 126.1), C-10 (δ_C 133.6), and C-8 (δ_C 151.5) (Fig. 5C). Oxidative degradation[6,27] established the absolute configuration at the stereocenter at C-1 as *R*. The ECD spectrum of the new alkaloid (Fig. 5E) was virtually opposite to that of ancistrobrevoline C (**16**), while resembling that of ancistrobrevolines A (**14**) and B (**15**) (see ESI†), hence establishing the absolute axial configuration as *P*. The new alkaloid consequently had the full absolute stereostructure **17** as presented in Fig. 5E. It was henceforth named ancistrobrevoline D.

Proposed biosynthetic origin of naphthylisoindolinone alkaloids

The structures of the discovered four novel alkaloids **14–17**, with their isoindolinone parts connected to the naphthalene moieties *via* a stereogenic axis, are unprecedented, and differ substantially from previously described artificial naphthylisoindolinones.[28–30] In the field of 'normal', amino-acid derived benzylisoquinoline alkaloids, some few other, yet naphthalene-devoid isoindolinones are known like aristoyagonine (**18**)[30–32] and aristolactam I (**19**)[30,33,34] (Fig. 6A). Biosynthetically, **18** and **19** are assumed to be formed from the corresponding benzyltetrahydroisoquinoline alkaloids, by 3,4-dioxygenation, followed by a benzilic acid rearrangement, with loss of a carbon atom and ring contraction.[30–34]

In an analogous way, the four novel naphthylisoindolinones **14–17** (general partial structure **IV**, see Fig. 6B) might arise from the respective naphthyltetrahydroisoquinoline alkaloids **I**, *via* the corresponding 3,4-diketones **III** – yet with the additional

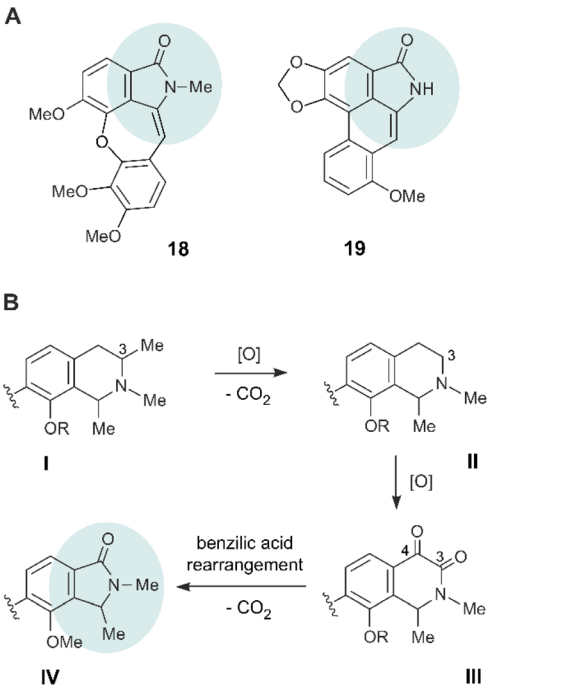

Fig. 6 (A) Structures of the conventional, naphthalene-devoid isoindolinones, aristoyagonine (**18**) and aristolactam (**19**). (B) From 'normal' naphthyltetrahydroisoquinolines (**I**) to ancistrobrevolines (**IV**): Proposed biosynthetic pathway, with oxidation, decarboxylation, and ring contraction reactions.

necessity of eliminating the methyl group at C-3, maybe *via* **II**, or possibly *via* the 3-oxo analogues. The loss of the C-3 methyl group might occur by a stepwise oxidation to the respective carboxylic acid followed by decarboxylation. A similar elimination of a *C*-methyl group in naphthylisoquinoline alkaloids had already been observed at C-1 (see the structure of 1-*nor*-8-*O*-demethylancistrobrevine H, **12**, in Fig. 1), as found to be produced by the same plant, *A. abbreviatus*,[18] and also oxygenations at Me-3 (see ref. 5, 35 and 36) and at C-4 (see ref. 5, 37 and 38) are known to occur in the biosynthesis of naphthylisoquinoline alkaloids. As in the case of **18** and **19**, the resulting diketones **III** could then undergo a benzilic acid rearrangement, with loss of CO_2, to provide the isoindolinone unit **IV**.

Cytotoxic activity of ancistrobrevolines A and B against breast and lung cancer cells

Some of the mono- and dimeric naphthylisoquinoline alkaloids isolated from the West African liana *A. abbreviatus* display strong cytotoxic activities against various cancer cell lines, among them multiple myeloma,[9,39] leukemia,[16,39] cervical,[15,18,40] fibrosarcoma,[17] colon,[17] and pancreatic[14,15,40] cancer cells. Investigations regarding the specificity and effectiveness of the compounds on the viability of those cancer cells indicated that the alkaloids may have a substantial therapeutic potential and can thus be regarded as promising candidates for drug development.

And only recently, dioncophylline A (**5**), a main constituent of *A. abbreviatus*, and related compounds have been reported to exhibit pronounced antiproliferative activities in the submicromolar range against two breast cancer cell lines, MCF-7 and MDA-MB-231.[41] Breast[42,43] and lung[44,45] cancer are among the most commonly diagnosed lethal cancer types worldwide. Although the death rate caused by cancer has been decreasing over the past years,[46] as a result of improved diagnostic and therapeutic approaches to many cancer types, treatment of lung and breast cancer still suffers from a poor prospect to completely eradicate the tumor cells, which in turn leads to a recurrent and metastatic manifestation of the disease, and thus to high mortality rates.[42–48] Therefore, the search for novel therapeutic agents to efficiently combat lung and breast cancer cells still remains an important task.

Given the pronounced antiproliferative activities of some of the naphthylisoquinoline alkaloids such as dioncophylline A (**5**),[17,39,41] jozimine A_2 (**11**),[17,40] or ancistrobrevidine C (**8**),[15] with their usual six-membered heterocyclic ring system, it seemed rewarding to likewise study the cytotoxic potential of the new ring-contracted naphthylisoindolinones. This was also promising in view of the fact that aristolactams (Fig. 6A) and some of their non-natural analogues,[28,33] all equipped with an isoindolinone moiety similar to the one of ancistrobrevolines A–D (**14–17**), are known to exhibit remarkable anticancer properties, too.[34,49,50]

We here, therefore, report on the evaluation of ancistrobrevolines A (**14**) and B (**15**) for their growth-inhibitory effects against MCF-7 breast adenocarcinoma cells and against the non-small cell lung cancer (NSCLC) cell line A549. Due to the lack of isolated material of ancistrobrevines C (**16**) and D (**17**), only **14** and **15** were assessed.

These two alkaloids exhibited only low cytotoxic effects against MCF-7 breast cancer cells, as determined by the MTT assay (see Experimental Section). The results showed that exposure of MCF-7 cells to varying concentrations (10, 30, 50, 70, and 100 μM) of **14** and **15** resulted in growth-inhibitory activities of 19-38% (for **14**) and 3.7–43% (for **15**) (see Table 2). Although **14** and **15** did not reach the pronounced growth-inhibitory activities of the previously investigated naphthylisoquinoline alkaloids on breast cancer cells,[41] the results are important contributions to our ongoing investigations on structure–activity (SAR) relationships.

Against A549 lung cancer cells, the cytotoxic activities of **14** and **15** were significantly higher, reaching *ca.* 8–72% and 36–68%, respectively (see Table 3), with IC_{50} values of 34.6 μM (for **14**) and 9.05 μM (for **15**) (Fig. 7). Thus, the IC_{50} value of ancistrobrevoline B (**15**) was markedly lower than that of ancistrobrevoline A (**14**), showing a higher sensitivity of A549 lung cancer cells to the growth inhibition induced by **15**, which further evidenced the pronounced structure–function diversity in naphthylisoquinoline alkaloids. Studies on the immortalized human mammary epithelial cell line MCF-10A[51] revealed ancistrobrevoline B (**15**) to display moderate cytotoxicity on these non-tumorigenic cells, which led to a selectivity index of 1.4 regarding the A549 cancer cell line, whereas ancistrobrevoline A (**14**) showed no selectivity towards the cancer cells compared to the normal epithelial MCF-10A cells (SI ≈ 1).

Cytotoxic activity of ancistrobrevolines A and B against breast and lung cancer cells

The manifestation of breast cancer is strongly associated with the occurrence of a small atypical population of tumor-initiating cells that possess the capacity of unlimited propagation and multipotent differentiation.[52–54] These cancer-stem-like cells have been identified in a variety of tumors and are under suspicion to be a causative factor of tumor growth and metastasis, eventually facilitating resistance to chemotherapies, and thus, leading to treatment failure and tumor recurrence.[55] Therefore, targeting these cancer stem cells in breast cancer has become a promising approach.[56]

Cultivation of human breast epithelial adenocarcinoma cells MCF-7 under non-adherent non-differentiating conditions as described in the Experimental section results in the generation

Table 2 Concentration-dependent cytotoxic activity of ancistrobrevolines A (**14**) and B (**15**) against breast cancer cells (MCF-7)

	Cytotoxicity ± SD[a] (%)				
Compound	10 μM	30 μM	50 μM	70 μM	100 μM
14	19.1 ± 22.7	25.3 ± 17.0	27.1 ± 6.82	28.5 ± 12.2	37.7 ± 12.7
15	3.68 ± 11.5	17.6 ± 31.5	34.0 ± 8.47	37.4 ± 13.0	43.0 ± 6.73

[a] The results are shown as mean values ± standard deviation (SD); the experiments were done in triplicate ($n = 3$).

Table 3 Concentration-dependent antiproliferative activity of ancistrobrevolines A (**14**) and B (**15**) against lung cancer cells (A549)

	Cytotoxicity ± SD (%)[a]				
Compound	10 μM	30 μM	50 μM	70 μM	100 μM
14	8.27 ± 10.3	26.4 ± 4.01	54.3 ± 3.47	58.0 ± 3.66	72.7 ± 2.88
15	36.4 ± 9.62	61.9 ± 2.11	63.8 ± 9.52	64.0 ± 1.69	68.3 ± 3.88

[a] The results are shown as mean values ± standard deviation (SD); the experiments were done in triplicate ($n = 3$).

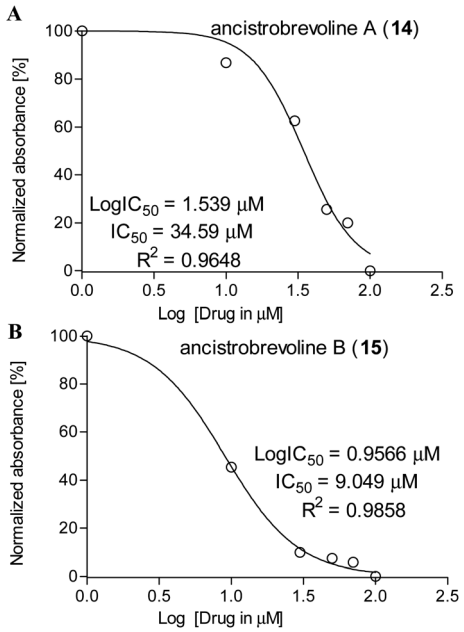

Fig. 7 Treatment of lung cancer (A549) cells with ancistrobrevolines A (**14**) and B (**15**). Determination of IC_{50} and log IC_{50} values, and regression analysis of the effects of (A) **14** and (B) **15** (10, 30, 50, 70, and 100 μM each) on the A549 cells after 48 h of incubation; the results are expressed as mean ± SD.

of discrete clusters of spheroids, termed mammospheres (Fig. 8A), which undergo asymmetric division and self-renewal, making them aggressive and highly metastatic.[57,58] Before this background, we studied the effect of ancistrobrevines A (**14**) and B (**15**) on the sphere formation potential of MCF-7 cells after exposure to 10, 30, 50, 70, and 100 μM of the new naphthylisoindolinone alkaloids. After 5 d of treatment, the size of the spheroids was captured using a phase-contrast microscope. As shown in Fig. 8, compounds **14** and **15** significantly reduced the size of the spheres in MCF-7 culture compared to the non-treated control group, where large spheroids were observed. A dose-dependent spheroid inhibitory activity of ancistrobrevolines A (**14**) and B (**15**) was found in MCF-7-derived mammospheres. The results indicate the reduction of stemness and self-renewal of MCF-7 cells in the presence of **14** and **15**.

Experimental

General experimental procedures

Optical rotations were recorded using a JASCO P-1020-polarimeter (JASCO, Gross-Umstadt, Germany) operating with a sodium light source ($\lambda = 589$ nm). UV spectra were measured on a Shimadzu UV-1800 spectrophotometer, and ECD spectra were recorded under nitrogen atmosphere on a JASCO J-715 spectrometer at room temperature, using a standard cell (0.02 cm), then processed using the SpecDis software.[59,60] IR spectra were measured on a JASCO FT/IR-410 spectrometer. 1D and 2D NMR spectra were taken on a Bruker DMX 600 instrument at ambient temperature, using methanol-d_4 as the solvent, with the ^{1}H and ^{13}C signals of the solvent (δ_H 3.31 and δ_C 49.15 ppm) as the internal reference. Chemical shifts (δ) are given in parts per million (ppm), and coupling constants (J) are reported in Hertz (Hz). Multiplicities of NMR signals are denoted as singlet (s), doublet (d), doublet of doublets (dd), or quartet (q). Spectra were processed using an the MestReNova NMR (Mestrelab

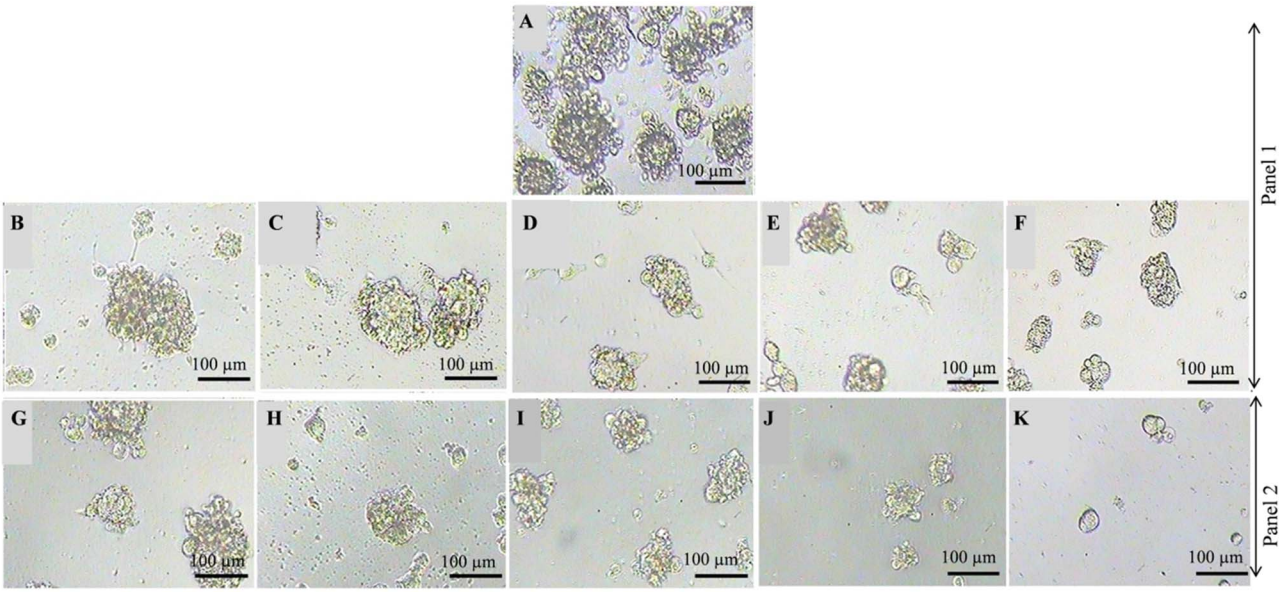

Fig. 8 Cytotoxic effects of ancistrobrevolines A (**14**) and B (**15**) on the formation of MCF-7-derived breast cancer stem-like cells (mammosphere). (A) Mammospheres derived from untreated MCF-7 cells as a control. (B–F) MCF-7 cells derived from mammospheres treated with **14** at concentrations of 10 (B), 30 (C), 50 (D), 70 (E), and 100 μM (F). (G-K) MCF-7 cells derived from mammospheres treated with **15** at concentrations of 10 (G), 30 (H), 50 (I), 70 (J), and 100 μM (K). The mammospheres were cultured for 5 d to form spheres in ultra-low attachment surface plates. The images of the mammospheres were taken at 10 × resolution using phase-contrast microscopy.

Research) software. HRESIMS spectra were acquired on a Bruker Daltonics micrOTOF-focus mass instrument. GC-MSD analysis was done on a GCMS-QP 2010SE System (Shimadzu). Preparative HPLC was accomplished on a JASCO System (PU-1580 Plus) in combination with a PDA detector at 195–650 nm (JASCO MD-2010 Plus diode array detector). For the isolation and purification of the constituents of the root bark extracts, a SymmetryPrep C_{18} column (19 × 300 mm, 7 μm, Waters) was used, applying a flow rate of 10 mL min^{-1}; mobile phases: (A) 90% H_2O with 10% CH_3CN (0.05% trifluoroacetic acid) and (B) 90% CH_3CN with 10% H_2O (0.05% trifluoroacetic acid). For further purification, a Waters X-Select HSS PFP column (10 × 250 mm, 5 μm) was applied; mobile phases: (A) 90% H_2O with 10% CH_3OH (0.05% trifluoroacetic acid) and (B) 90% CH_3OH with 10% H_2O (0.05% trifluoroacetic acid).

Plant material

Roots of *Ancistrocladus abbreviatus* Airy Shaw (Ancistrocladaceae) were collected by one of us (late Prof. L. Aké Assi) in May 1996, in the Parc National de Taï, in the Southwest of the Ivory Coast. A voucher specimen (no. 3) has been deposited at the Herbarium Bringmann, Institute of Organic Chemistry, University of Würzburg.

Chemical and reagents

For the purification of the plant fractions by preparative HPLC, HPLC-grade solvents MeCN, MeOH, purchased from Sigma-Aldrich, were utilized. Spectroscopic-grade methanol was used for the ECD and UV measurements of the pure alkaloids. Ultrapure water for HPLC was obtained from an Elga Purelab Classic System. (*S*)-MTPA used for the degradation was purchased from Sigma-Aldrich (Steinheim, Germany).

Dulbecco's Modified Eagle Medium (DMEM), fetal bovine serum (FBS), trypsin, penicillin, streptomycin, horse serum, epidermal growth factor (EGF), fibroblast growth factor (FGF), B-27 supplements, hydrocortisone, and insulin were purchased from Thermo Fisher Scientific (Waltham, MA, USA). For cell proliferation assays, 3-(4,5-dimethylthiazol-2-yl)-2,5-diphenyltetrazolium bromide (MTT) and cholera toxin were obtained from Sigma-Aldrich (St. Louis, MO, USA).

Extraction and purification of naphthylisoindolinones

The air-dried powdered root bark material of *A. abbreviatus* (*ca.* 420 g) was macerated in methanol (2 × 3 L) at 40 °C, followed by ultrasonication for 1 h. The extract was filtered, and the solvent was evaporated under reduced pressure to give a brownish solid residue, which was re-dissolved in 90% aqueous methanol and partitioned with *n*-hexane. The aqueous methanolic layer was dried under reduced pressure to yield 17.5 g of an alkaloid-rich fraction, which was directly subjected to fractionation over a silica gel column using a linear solvent system consisting of CH_3OH and CH_2Cl_2 with a gradient increase of CH_3OH (0 → 90%), giving rise to five naphthylisoindolinone-enriched fractions (F_1–F_5). The alkaloid-containing subfractions were purified on the X-Select HSS PFP column by applying the following method: 0 min: 68% B, 38 min: 88% B, affording 0.7 mg of ancistrobrevoline C (**16**) (retention time 22.0 min), 0.6 mg of ancistrobrevoline B (**15**) (retention time 25.3 min), 0.5 mg of ancistrobrevoline D (**17**) (retention time 26.4 min), and 1.1 mg of ancistrobrevoline A (**14**) (retention time 28.1 min).

Ancistrobrevoline A (14). Yellow, amorphous powder; $[\alpha]_D^{23}$ +11.5 (*c* 0.05, MeOH); UV/Vis (MeOH) λ_{max} (log ε) 196 (4.1), 213 (3.7), 229 (3.6), 261 (3.0), 306 (3.0) nm; ECD (*c* 0.10; MeOH) λ_{max} (log ε) 213 (−2.7), 235 (−1.1), 249 (+1.5), 326 (+0.1) cm^2 mol^{-1}; IR (ATR) ν_{max} 3400, 2967, 2929, 1673, 1585, 1463, 1421, 1383, 1198, 1132, 951, 808, 672 cm^{-1}; ^1H NMR and ^{13}C NMR data, see Table 1; HR-ESI-MS *m*/*z* 444.17711 $[M + Na]^+$ (calcd for $C_{25}H_{27}NNaO_5$, 444.17814).

Ancistrobrevoline B (15). Yellow, amorphous solid; $[\alpha]_D^{23}$ −8.3 (*c* 0.07, MeOH); UV/Vis (MeOH) λ_{max} (log ε) 196 (4.1), 213 (3.5), 227 (3.4), 261 (2.8), 306 (2.8) nm; ECD (*c* 0.10; MeOH) λ_{max} (log ε) 212 (−2.4), 232 (−1.1), 247 (+1.7), 301 (−0.1) cm^2 mol^{-1}; IR (ATR) ν_{max} 2965, 1678, 1587, 1463, 1428, 1383, 1196, 1135, 836, 803, 673 cm^{-1}; ^1H NMR and ^{13}C NMR data, see Table 1; HR-ESI-MS *m*/*z* 408.1815 $[M + H]^+$ (calcd for $C_{24}H_{26}NO_5$, 408.1805), and *m*/*z* 430.1611 $[M + Na]^+$ (calcd for $C_{24}H_{25}NNaO_5$, 430.1624).

Ancistrobrevoline C (16). Yellow, amorphous powder; $[\alpha]_D^{23}$ −18.9 (*c* 0.05, MeOH); UV/Vis (MeOH) λ_{max} (log ε) 197 (4.1), 215 (3.5), 228 (2.4), 261 (2.8), 304 (2.7) nm; ECD (*c* 0.10; MeOH) λ_{max} (log ε) 205 (−0.6), 225 (+1.5), 250 (−1.3), 300 (+0.09) cm^2 mol^{-1}; IR (ATR) ν_{max} 2927, 2850, 1675, 1589, 1459, 1387, 1264, 1200, 1135, 836, 805, 719 cm^{-1}; ^1H NMR and ^{13}C NMR data, see Table 1; HR-ESI-MS *m*/*z* 408.1797 $[M + H]^+$ (calcd for $C_{24}H_{26}NO_5$, 408.1805), and *m*/*z* 430.1608 $[M + Na]^+$ (calcd for $C_{24}H_{25}NNaO_5$, 430.1624).

Ancistrobrevoline D (17). Yellow, amorphous powder; $[\alpha]_D^{23}$ −24.0 (*c* 0.04, MeOH); UV/Vis (MeOH) λ_{max} (log ε) 197 (4.0), 229 (3.2), 295 (2.6), 334 (2.5) nm; ECD (*c* 0.10; MeOH) λ_{max} (log ε) 209 (+0.1), 226 (−2.7), 246 (+1.3), 286 (+0.08) cm^2 mol^{-1}; IR (ATR) ν_{max} 2969, 2850, 1680, 1594, 1459, 1327, 1204, 1134, 1075, 725, 672 cm^{-1}; ^1H NMR and ^{13}C NMR data, see Table 1; HR-ESI-MS *m*/*z* 400.1503 $[M + Na]^+$ (calcd for $C_{23}H_{23}NNaO_4$, 400.1519).

Oxidative degradation

The naphthylisoindolinone alkaloids **14–17** (*ca.* 0.5 mg each) were subjected to a ruthenium(VIII)-mediated periodate degradation,[6,27] followed by derivatization of the resulting amino acids with CH_3OH/HCl and (*R*)-α-trifluoromethylphenylacetylchloride [(*R*)-MTPA-Cl, prepared from (*S*)-MTPA]. The absolute configurations were assigned by GC on a dimethylpolysiloxane-coated capillary column coupled to a mass-selective detector and comparison with the corresponding derivatives of authentic amino acids of known absolute configuration.

Computational details

For the calculation of the ECD spectra, a simplified approach was selected. Only the main conformers of the possible configurations of compound **14** were optimized with B3LYP-D3//def2-TZVP.[61–63] The conformational freedom of the methoxy groups was not taken into account because their influence on the ECD should be negligible. Excited states results were achieved utilizing TDωB97XD3/def2-TZVP(-f).[64,65] All calculations

were done using ORCA 4.1.0.2.[66] For processing of the data, SpecDis 1.71 was used[59,60] with a UV shift of 18 nm, finally providing the computed ECD spectra, which were compared with the experimental one of **14**.

Cell culture

Human breast (MCF-7) and lung (A549) cancer cells were purchased from the National Centre for Cell Sciences, Pune, India. Normal, non-tumoral breast cells (MCF-10A) were from ATTC, University Boulevard, Manassas, VA, USA. Breast and lung cancer cells were cultured in DMEM supplemented with 10% (v/v) FBS (heat-inactivated), 2 mM L-glutamine, 100 μg mL^{-1} of streptomycin and 100 U mL^{-1} of penicillin. The normal breast cells (MCF-10A) were maintained in DMEM/F12 media supplemented with FBS (10%), horse serum (5%), cholera toxin (100 ng mL^{-1}), EGF (20 ng mL^{-1}), hydrocortisone (0.5 mg mL^{-1}), and insulin (10 μg mL^{-1}) and incubated at 37 °C and 5% CO_2.

Cytotoxicity study using the MTT assay

Approximately 10^4 cells/well were seeded in 96-well plates and kept in the incubator at 37 °C and 5% CO_2. The cells were kept overnight to allow them to adhere and were then fed with fresh medium containing different concentrations (10, 30, 50, 70, and 100 μM) of the test compounds, ancistrobrevolines A (**15**) and B (**16**). After incubation for 48 h, cell viability was assessed using the MTT assay.[67] At the stipulated time following the treatment of the test sample, medium was aspirated; MTT (5 mg mL^{-1}) was added in each well and incubation was continued at 37 °C for 2 h. The plates were spun, supernatants were discarded, and purple-colored precipitates of formazan were dissolved in 100 μL of dimethylsulfoxide (DMSO). The color absorbance was recorded at 590 nm using a microplate reader (BioTek Instruments, Inc. USA). IC_{50} calculations and regression analysis were performed using the GraphPad Prism 5.0 software.

The selectivity index (SI) of the test compounds was calculated using the following equation, where MCF-10A represents human normal cells, while A549 denotes lung cancer cells: $SI = IC_{50\ \text{normal cells}}/IC_{50\ \text{cancer cells}}$. The IC_{50} value indicates the concentration of the test drug required for 50% inhibition of the cancer cells. SI values > 1 indicate that the compound is selective against the respective cancer cells.[68]

Mammosphere formation and drug treatment

Mammospheres derived from MCF-7 cells were formed by seeding the cells in 6-well ultra-low-attachment surface plates (Corning, Tewksbury, MA, USA) at a density of 2×10^4 cells/well and cultured in serum-free DMEM-Ham's F12 nutrient mixture (1 : 1, v/v), supplemented with 5 mg mL^{-1} insulin, 0.5 mg mL^{-1} hydrocortisone, 2% B-27 supplements, 10 ng mL^{-1} fibroblast growth factor, and 20 ng mL^{-1} epidermal growth factor. The cells were incubated at 37 °C and 5% CO_2 for 5 d to form mammospheres.[69] To study the effect of ancistrobrevolines A (**14**) and B (**15**) on mammosphere formation, the cells were treated with different concentrations (10, 30, 50, 70, and 100 μM) of the agents and then allowed to form spheres for the next 5 d. The compound solutions were prepared using DMSO with its final non-toxic concentration (0.1%). An equal amount of DMSO was added to the non-treated control group. After 5 d, the mammospheres were photographed using phase-contrast microscopy, and the images were analyzed using the ImageJ analysis software.[69]

Conclusions

This paper describes the discovery of a structurally novel subclass of naphthylisoquinoline-related alkaloids, bearing a heterocyclic moiety that is ring-contracted to an isoindolinone entity. The results further highlight the "chemical creativity" of *A. abbreviatus* and demonstrate the outstanding phytochemical diversity of this productive West African liana. Already at the level of 'normal', standard-type naphthyltetrahydroisoquinoline alkaloids, the plant shows a remarkably broad variability,[5,10,11,13,14,17] with no less than four out of seven known *C*,*C*-coupling types (5,1′, 7,1′, 5,8′, and 7,8′) and an otherwise very rare stereo-diversity, producing all four possible stereochemical combinations at C-1/C-3 (*i.e.* *S*,*S*, *S*,*R*, *R*,*S*, and *R*,*R*) (Fig. 1). In addition, it is the only plant that contains all four possible subclasses of naphthylisoquinoline alkaloids,[5,17] namely Ancistrocladaceae- (6-OR, 3*S*), Dioncophyllaceae- (6-H, 3*R*), hybrid- (6-OR, 3*R*), and inverse hybrid-type (6-H, 3*S*) representatives, as outlined in Fig. 1.

Moreover, *A. abbreviatus* excels by the highest number of metabolic follow-up variations, resulting from – mostly oxidative – secondary modifications. Besides the phenol-oxidative coupling *via* the naphthalene portion, *e.g.* to give jozimine A_2 (**11**),[17] with its three stereogenic axes, and a nearly complete series of its numerous atropo-diastereomers, it is the only plant that produces naphthylisoquinoline alkaloids whose isocyclic moiety is further oxygenated to form an *ortho*-naphthoquinone as in ancistrobreviquinone A (**10**).[15]

Even more thrilling are the downstream variations of the tetrahydroisoquinoline portion, which can be dehydrogenated leading to the otherwise less frequently occurring 3,4-dihydroisoquinolines and to the (normally very rare) fully dehydrogenated naphthylisoquinoline alkaloids, with no less than seven representatives. Totally unprecedented even is the occurrence of 1-demethylated naphthylisoquinolines like 1-*nor*-8-*O*-demethylancistrobrevine H (**12**)[18] and ring-cleaved representatives like ancistrosecoline D (**13**)[18] (Fig. 1) – and, as described here, the discovery of oxidatively ring-contracted alkaloids, delivering new molecular scaffolds within the class of naphthylisoquinoline alkaloids.

These first four naphthylisoindolinones, ancistrobrevolines A–D (**14–17**), are all *N*-methylated, and they are all fully *O*-methylated in the naphthalene part and all are *R*-configured at C-1. In that respect they fit with the structural properties of the presumable precursors to **14**, **15**, **16**, and **17**, *viz.*, ancistrobrevine A (**1**), its 6-*O*-demethyl analogue **2**, ancistrobrevine D (**3**), and *N*-methyldioncophylline A (**5**) (Fig. 1), respectively, which, in agreement with our biosynthetic concept, all co-occur in *A. abbreviatus*, where they are even among the main alkaloids. Despite their structural similarities, the new metabolites do vary

by their oxygenation degree at C-6, by the *O*-methylation degree at C-8, and by the stereo-orientation at the biaryl axis. This suggests that the structural requirements for the ring contraction are not particularly specific, evidencing that isoindolinone formation in naphthylisoquinoline alkaloids is possibly a more general principle. The work shows that naphthylisoquinoline alkaloids are not just metabolically stable bioactive end products, but can also be substrates for further – mainly oxidative – modifications.

Among all investigated naphthylisoquinoline-producing plants, *A. abbreviatus* shows the broadest diversity of secondary metabolites. It thus occupies a phytochemically – and phylogenetically – outstanding position within the Ancistro-cladaceae family, with a close relationship to Dioncophyllaceae lianas such as *Triphyophyllum peltatum* on the one hand and to geographically neighboring West and Central African Ancistrocladaceae plants on the other. Ancistrobrevolines A (**14**) and B (**15**) exhibited moderate antiproliferative activities against breast (MCF-7) and lung (A549) cancer cell lines. Furthermore, **14** induced a significant reduction of the formation of highly metastatic spheroid clusters in breast cancer-derived cancer-stem-like cells, worth further, more in-depth investigations on the antitumoral potential of naphthylisoquinoline alkaloids. The results presented here render phytochemical studies on the numerous further, as yet unidentified, trace compounds of *Ancistrocladus* plants and their biological evaluation rewarding goals.

Conflicts of interest

There are no conflicts to declare.

Acknowledgements

This work was supported by the Deutsche Forschungsgemeinschaft (DFG, Research Grant Br 699/14-2 "Molecular Phylogeny and Chemotaxonomy of the Ancistrocladaceae Plant Family") and by a grant from the German Academic Exchange Service (Deutscher Akademischer Austauschdienst, DAAD) to one of us (S. F.). This publication was supported by the Open Access Publication Fund of the University of Würzburg. We thank Dr M. Grüne and Mrs. P. Altenberger for the NMR measurements, and Dr M. Büchner and Dr J. Adelmann for the MS analyses, all from the University of Würzburg. S. K. acknowledges DST-India for providing a DST-FIST grant to the Department of Biochemistry, Central University of Punjab, Bathinda, India.

Notes and references

1 C. M. Taylor, R. E. Gereau and G. M. Walters, *Ann. Mo. Bot. Gard.*, 2005, **92**, 360–399.
2 M. Cheek, *Kew Bull.*, 2000, **55**, 871–882.
3 H. K. Airy Shaw, *Kew Bull.*, 1949, **4**, 68–69.
4 H. K. Airy Shaw, *Kew Bull.*, 1950, **5**, 147–150.
5 G. Bringmann and F. Pokorny, The naphthylisoquinoline alkaloids, in *The Alkaloids*, ed. G. A. Cordell, Academic Press Inc, New York, 1995, vol. 46, pp. 127–271.
6 B. K. Lombe, D. Feineis and G. Bringmann, *Nat. Prod. Rep.*, 2019, **36**, 1513–1545.
7 N. Tajuddeen and G. Bringmann, *Nat. Prod. Rep.*, 2021, **38**, 2154–2186.
8 S. R. M. Ibrahim and G. A. Mohamed, *Fitoterapia*, 2015, **106**, 194–225.
9 X. F. Shang, C. J. Yang, S. L. Morris-Natschke, J. C. Li, X. D. Yin, Y. Q. Liu, J. W. Peng, M. Goto, J. Y. Zhang and K. H. Lee, *Med. Res. Rev.*, 2020, **40**, 2212–2289.
10 G. Bringmann, D. Lisch, H. Reuscher, L. Aké Assi and K. Günther, *Phytochemistry*, 1991, **30**, 1307–1310.
11 G. Bringmann, R. Zagst, H. Reuscher and L. Aké Assi, *Phytochemistry*, 1992, **31**, 4011–4014.
12 G. Bringmann, F. Pokorny, M. Stäblein, M. Schäffer and L. Aké Assi, *Phytochemistry*, 1993, **33**, 1511–1515.
13 G. Bringmann, R. Weirich, D. Lisch and L. Aké Assi, *Planta Med.*, 1992, **58**, A703–A704.
14 S. Fayez, D. Feineis, L. Aké Assi, M. Kaiser, R. Brun, S. Awale and G. Bringmann, *Fitoterapia*, 2018, **131**, 245–259.
15 S. Fayez, A. Cacciatore, S. Sun, M. Kim, L. Aké Assi, D. Feineis, S. Awale and G. Bringmann, *Bioorg. Med. Chem.*, 2021, **30**, 115950.
16 S. Fayez, D. Feineis, L. Aké Assi, E. J. Seo, T. Efferth and G. Bringmann, *RSC Adv.*, 2019, **9**, 15738–15748.
17 S. Fayez, J. Li, D. Feineis, L. Aké Assi, M. Kaiser, R. Brun, M. A. Anany, H. Wajant and G. Bringmann, *J. Nat. Prod.*, 2019, **82**, 3033–3046.
18 S. Fayez, T. Bruhn, D. Feineis, L. Aké Assi, S. Awale and G. Bringmann, *J. Nat. Prod.*, 2020, **83**, 1139–1151.
19 G. Bringmann, C. Günther, M. Ochse, O. Schupp and S. Tasler, in *Progress in the Chemistry of Organic Natural Products*, ed. W. Herz, H. Falk, G. W. Kirby and R. E. Moore, Springer, Wien, New York, 2001, vol. 82, pp. 111–124.
20 J. E. Smyth, N. M. Butler and P. A. Keller, *Nat. Prod. Rep.*, 2015, **32**, 1562–1583.
21 H. K. Airy Shaw, *Kew Bull.*, 1951, **6**, 327–347.
22 S. Porembski and W. Barthlott, in *The Families and Genera of Vascular Plants. V. Flowering Plants – Dicotyledons, Malvales, Capparales and Non-betain Caryophyllales*, ed. K. Kubitzki and C. Bayer, Springer, Heidelberg, 2002, vol. 5, pp. 178–181.
23 G. Bringmann, G. François, L. Aké Assi and J. Schlauer, *Chimia*, 1998, **52**, 18–28.
24 G. Bringmann, M. Rübenacker, J. R. Jansen, D. Scheutzow and L. Aké Assi, *Tetrahedron Lett.*, 1990, **31**, 639–642.
25 G. Bringmann, J. R. Jansen, H. Reuscher, M. Rübenacker, K. P. Peters and H. G. von Schnering, *Tetrahedron Lett.*, 1990, **31**, 643–646.
26 For better comparability, the atom numbering follows the one applied for normal, intact naphthylisoquinolines, as also previously used for the *seco*-type ancistrosecolines[18] like *e.g.*, compound **13**.
27 G. Bringmann, R. God and M. Schäffer, *Phytochemistry*, 1996, **43**, 1393–1403.

28 T. Wu, Y. Wang, L. Li, J. Feng, Y. Liu, P. Ren and Y. Liu, *US pat*. 2017/055656, WO 2018/068017 A1 12.04.2018.
29 M. Urbano, E.-K. Kim, C. Chen, Q. Li, J. Ayers, K. Nakamura, X. Zhu, H. Rosen, J. Rosenblum, M. C. Zhang, Y. Liu and M. Ueno, *US pat*. 2020/015683, WO 2020/160151 A1 06.08.2020.
30 K. Speck and T. Magauer, *Beilstein J. Org. Chem.*, 2013, **9**, 2048–2078.
31 M. J. Campello, L. Castedo, D. Dominguez, A. R. De Lera, J. M. Saá, R. Suau, E. Tojo and M. C. Vidal, *Tetrahedron Lett.*, 1984, **25**, 5933–5936.
32 E. Tojo, D. Dominguez and L. Castedo, *Phytochemistry*, 1991, **30**, 1005–1010.
33 V. Kumar, Poonam, A. K. Prasad and V. S. Parmar, *Nat. Prod. Rep.*, 2003, **20**, 565–583.
34 J. Michel, M. J. Ingrouille, M. S. J. Simmonds and M. Heinrich, *Nat. Prod. Rep.*, 2014, **31**, 676–693.
35 G. Bringmann, M. Dreyer, H. Rischer, K. Wolf, H. A. Hadi, R. Brun, H. Meimberg and G. Heubl, *J. Nat. Prod.*, 2004, **67**, 2058–2062.
36 G. Bringmann, R. Seupel, D. Feineis, M. Xu, G. Zhang, J. Wu, M. Kaiser, R. Brun, E.-J. Seo and T. Efferth, *Fitoterapia*, 2017, **121**, 76–85.
37 G. Bringmann, T. Ortmann, R. Zagst, B. Schöner, L. Aké Assi and C. Burschka, *Phytochemistry*, 1992, **31**, 4015–4018.
38 G. Bringmann, C. Günther, W. Saeb, J. Mies, R. Brun and L. Aké Assi, *Phytochemistry*, 2000, **54**, 337–346.
39 J. Li, R. Seupel, D. Feineis, V. Mudogo, M. Kaiser, R. Brun, D. Brünnert, M. Chatterjee, E.-J. Seo, T. Efferth and G. Bringmann, *J. Nat. Prod.*, 2017, **80**, 443–458.
40 J. Li, R. Seupel, T. Bruhn, D. Feineis, M. Kaiser, R. Brun, V. Mudogo, S. Awale and G. Bringmann, *J. Nat. Prod.*, 2017, **80**, 2807–2817.
41 P. P. Kushwaha, A. K. Singh, S. Prajapati, M. Shuaib, S. Fayez, G. Bringmann and S. Kumar, *Toxicol. Appl. Pharmacol.*, 2020, **409**, 115297.
42 N. Harbeck, F. Penault-Llorca, J. Cortes, M. Gnant, N. Houssami, P. Poortmans, K. Ruddy, J. Tsang and F. Cardoso, *Nat. Rev. Dis. Primers*, 2019, **5**, 66.
43 S. Łukasiewicz, M. Czeczelewski, A. Forma, J. Baj, R. Sitarz and A. Stanisławek, *Cancers*, 2021, **12**, 4287.
44 A. A. Thai, B. J. Solomon, L. V. Sequist, J. F. Gainor and R. S. Heist, *Lancet*, 2021, **398**, 535–554.
45 H. Lemjabbar-Alaoui, O. Hassan, Y. W. Yang and P. Buchanan, *Biochim. Biophys. Acta*, 2015, **1856**, 189–210.
46 R. L. Siegel, K. D. Miller, H. E. Fuchs and A. Jemal, *Ca-Cancer J. Clin.*, 2022, **72**, 7–33.
47 A. G. Waks and E. P. Winer, *JAMA*, 2019, **32**, 288–300.
48 M. Yuan, L. L. Huang, J. H. Chen, J. Wu and Q. Xu, *Signal Transduct. Target. Ther.*, 2019, **4**, 61.
49 W. Chanakul, P. Tuchinda, N. Anantachoke, M. Pohmakotr, P. Piyachaturawat, S. Jariyawat, K. Suksen, T. Jaipetch, N. Nuntasaen and V. Reutrakul, *Fitoterapia*, 2011, **82**, 964–968.
50 S. Nayyatip, P. Thaichana, M. Buayairaksa, W. Tuntiwechapikul, P. Meepowpan, N. Nuntasaen and W. Pompimon, *Int. J. Mol. Sci.*, 2012, **13**, 5010–5018.
51 S. Liu and Y. C. Lin, *Breast J.*, 2004, **10**, 514–521.
52 M. J. Grimshaw, L. Cooper, K. Papazisis, J. A. Coleman, H. R. Bohnenkamp, L. Chiapero-Stanke, J. Taylor-Papdimitriou and J. M. Burchel, *Breast Cancer Res.*, 2017, **10**, R52.
53 S. Yousefnia, K. Ghaedi, F. S. Forootan and M. H. N. Esfahani, *Tumor Biol.*, 2019, **41**, 1–14.
54 Y. Lombardo, A. de Giorgio, C. R. Coombes, J. Stebbing and L. Castellano, *J. Visualized Exp.*, 2015, **97**, e52671.
55 K. S. Prajapati, M. Shuaib, S. Gupta and S. Kumar, *Mol. Carcinog.*, 2022, **61**, 876–889.
56 M. Al-Hajj, M. S. Wicha, A. Benito-Hernandez, S. J. Morrison and M. F. Clarke, *Proc. Natl. Acad. Sci. U. S. A.*, 2003, **100**, 3983–3988.
57 C. T. Jordan, M. L. Guzman and M. Noble, *N. Engl. J. Med.*, 2006, **355**, 1253–1261.
58 A. Schulenburg, H. Ulrich-Pur, D. Thurnher, B. Erovic, S. Florian, W. R. Sperr, K. Kalhs, P. Marian, F. Wrba, C. C. Zielinkski and P. Valent, *Cancer*, 2006, **107**, 2512–2520.
59 T. Bruhn, A. Schaumlöffel, Y. Hemberger and G. Bringmann, *Chirality*, 2013, **25**, 243–249.
60 T. Bruhn, A. Schaumlöffel, Y. Hemberger and G. Pescitelli, *SpecDis, Version 1.71*, **https://www.specdis-software.jimdo.com**, Berlin, Germany, 2017.
61 S. Grimme, J. Antony, S. Ehrlich and H. Krieg, *J. Chem. Phys.*, 2010, **132**, 154104–154119.
62 F. Weigend and R. Ahlrichs, *Phys. Chem. Chem. Phys.*, 2005, **7**, 3297–3305.
63 F. Weigend, *Phys. Chem. Chem. Phys.*, 2006, **8**, 1057–1065.
64 U. Ekström, L. Visscher, R. Bast, A. J. Thorvaldsen and K. Ruud, *J. Chem. Theory Comput.*, 2010, **6**, 1971–1980.
65 Y. S. Lin, G. D. Li, S. P. Mao and J. D. Chai, *J. Chem. Theory Comput.*, 2013, **9**, 263–272.
66 F. Neese, *Wiley Interdiscip. Rev.: Comput. Mol. Sci.*, 2018, **8**, e1327.
67 P. P. Kushwaha, P. S. Vardhan, P. Kapewangolo, M. Shuaib, S. K. Prajapati, A. K. Singh and S. Kumar, *Life Sci.*, 2019, **234**, 116783.
68 Y. Santiago-Vázquez, U. Das, A. Varela-Ramirez, S. T. Baca, Y. Ayala-Marin, C. Lema, S. Das, A. Baryyan, J. R. Dimmock and R. J. Aguilera, *Clin. Cancer Drugs*, 2016, **3**, 138–146.
69 P. P. Kushwaha, A. K. Singh, M. Shuaib, K. S. Prajapati, P. S. Vardhan, S. Gupta and S. Kumar, *Chem.-Biol. Interact.*, 2020, **328**, 109200.